

# Adipose-Derived Mesenchymal Stromal Cells Improve the Healing of Colonic Anastomoses Following High Dose of Irradiation Through Anti-Inflammatory and Angiogenic Processes

Cell Transplantation  
2017, Vol. 26(12) 1919–1930  
© The Author(s) 2018  
Reprints and permission:  
sagepub.com/journalsPermissions.nav  
DOI: 10.1177/0963689717721515  
journals.sagepub.com/home/cti  
 SAGE

Dirk Van de putte<sup>1</sup>, Christelle Demarquay<sup>2</sup>, Elke Van Daele<sup>1</sup>, Lara Moussa<sup>2</sup>, Christian Vanhove<sup>3</sup>, Marc Benderitter<sup>2</sup>, Wim Ceelen<sup>1,4</sup>, Piet Pattyn<sup>1</sup>, and Noëlle Mathieu<sup>2</sup>

## Abstract

Cancer patients treated with radiotherapy (RT) could develop severe late side effects that affect their quality of life. Long-term bowel complications after RT are mainly characterized by a transmural fibrosis that could lead to intestinal obstruction. Today, surgical resection is the only effective treatment. However, preoperative RT increases the risk of anastomotic leakage. In this study, we attempted to use mesenchymal stromal cells from adipose tissue (Ad-MSCs) to improve colonic anastomosis after high-dose irradiation. MSCs were isolated from the subcutaneous fat of rats, amplified in vitro, and characterized by flow cytometry. An animal model of late radiation side effects was induced by local irradiation of the colon. Colonic anastomosis was performed 4 wk after irradiation. It was analyzed another 4 wk later (i.e., 8 wk after irradiation). The Ad-MSC-treated group received injections several times before and after the surgical procedure. The therapeutic benefit of the Ad-MSC treatment was determined by colonoscopy and histology. The inflammatory process was investigated using Fluorine-182-Fluoro-2-Deoxy-d-Glucose Positron Emission Tomography and Computed Tomography (<sup>18</sup>F-FDG-PET/CT) imaging and macrophage infiltrate analyses. Vascular density was assessed using immunohistochemistry. Results show that Ad-MSC treatment reduces ulcer size, increases mucosal vascular density, and limits hemorrhage. We also determined that 1 Ad-MSC injection limits the inflammatory process, as evaluated through <sup>18</sup>F-FDG-PET-CT (at 4 wk), with a greater proportion of type 2 macrophages after iterative cell injections (8 wk). In conclusion, Ad-MSC injections promote anastomotic healing in an irradiated colon through enhanced vessel formation and reduced inflammation. This study also determined parameters that could be improved in further investigations.

## Keywords

preoperative radiotherapy side effects, colonic anastomosis, adipose mesenchymal stromal cells, cellular therapy

## Introduction

Radiotherapy (RT) is used in at least 50% of cancer patients and approximately 25% of solid tumors undergo complete remission after RT.<sup>1</sup> Abdominal or pelvic RT is commonly accepted as a neoadjuvant, central adjuvant, or even palliative therapy in the treatment programs of colorectal,<sup>2,3</sup> urological,<sup>4</sup> and gynecological tumors. Healthy regions of the small intestine, colon, and rectum inevitably lie within the field of irradiation used to treat tumors in the abdominal or pelvic cavity. These healthy tissues are thus at risk of severe damage. Intestinal radiation toxicity is a complex and dynamic process involving stem cell depletion, endothelial cell activation, and chronic inflammation associated with

<sup>1</sup> Department of Pediatric and Gastrointestinal Surgery, Ghent University Hospital, Ghent, Belgium

<sup>2</sup> Institut de Radioprotection et de Sûreté Nucléaire (IRSN), Fontenay-aux-Roses, France

<sup>3</sup> Infinity lab, Ghent University Hospital, Ghent, Belgium

<sup>4</sup> Cancer Research Institute Ghent (CRIG), Ghent, Belgium

Submitted: May 04, 2017. Revised: June 21, 2017. Accepted: June 24, 2017.

### Corresponding Author:

Noëlle Mathieu, Institut de Radioprotection et de Sûreté Nucléaire (IRSN), PRP-HOM, SRBE, LR2I, Fontenay-aux-Roses, 92262, France.  
Email: noelle.mathieu@irsn.fr



Creative Commons CC BY-NC: This article is distributed under the terms of the Creative Commons Attribution-NonCommercial 4.0 License (<http://www.creativecommons.org/licenses/by-nc/4.0/>) which permits non-commercial use, reproduction and distribution of the work without further permission provided the original work is attributed as specified on the SAGE and Open Access pages (<https://us.sagepub.com/en-us/nam/open-access-at-sage>).

persistent oxidative stress, contributing to tissue fibrosis and leading to structural and functional alterations.<sup>5</sup> Chronic side effects are described in 5% and 10% of the patients treated by pelvic RT 5 and 10 years, respectively, after the end of their cancer treatment, and they are the cause of substantial long-term morbidity.<sup>6</sup> Despite the significant increase in cancer patient survival due to RT, radiation toxicity of normal tissue surrounding the tumor is clearly identified as a high-risk factor for postoperative complications,<sup>7,8</sup> including impaired bowel anastomotic healing. Preoperative RT is considered to be a risk factor for esophageal<sup>8</sup> and rectal<sup>9–11</sup> anastomotic healing. In the case of colorectal cancer as well as benign conditions or anomalies like diverticulitis or duplication cysts, anastomotic leakage during curative resection is still considered a major clinical problem since it is associated with high rates of morbidity and mortality. In the literature of the past 25 years, reported mortality has been as high as 33%.<sup>12</sup> The most important factor involved in anastomotic leakage is abnormal blood supply. Hypoxia could interfere with tissue viability, leading to tissue necrosis and, consequently, delayed healing. Ischemic wounds heal poorly and infect easily, exacerbating mucosal inflammation. Optimization of the healing processes is a central topic in surgical research. Attempts to enhance anastomotic healing included improvements in surgical techniques, various innovative sealing procedures, and use of various growth factors to stimulate the healing process.<sup>13</sup> However, the benefits of these treatments have not been tested in high-risk anastomoses, as during sepsis or after irradiation. Recent studies conclude that radiation therapy is an independent risk factor for anastomotic leakage.<sup>14</sup> Acute colorectal radiation toxicity (within 3 mo) is the result of crypt cell apoptosis leading to mucosal lesions with loss of epithelial barrier function. The increased mucosal permeability leads to nutrient and fluid loss and increased gut pathogen infiltration, exacerbating mucosal inflammation. Increased vascular permeability also contributes to infiltration of the injured mucosa by immune cells, mainly neutrophils and macrophages.<sup>15</sup> Delayed radiation colopathy is more complex, irreversible, often progressive, and characterized by mucosal atrophy, fibrosis of the colon wall, and microvascular sclerosis.<sup>16</sup> It is now recognized that the pathophysiology is not adequately explained by the target theory, where only the epithelium was thought to be responsible for acute toxicity, and both fibroblasts and endothelial cells for delayed toxicity. Enteric neuroimmune interactions, the colonic microbiota and microvasculature, composition of intraluminal contents, stem cell loss, and other factors are also involved in toxicity pathways. Anastomosis in an irradiated colon involves colonic wound healing and radio-induced inflammatory processes, fibrosis, and damage to the vascular network. Consequently, there is thought to be a high risk of leakage. In some patients, functional complications associated with the anatomy of the colon and rectum make it impossible to completely remove the irradiated area.

Adult mesenchymal stromal cells (MSCs) are self-renewing, easily expandable progenitor/stem cells. Their therapeutic effects in various diseases have been reported,<sup>17–23</sup> suggesting a potential use for MSCs in regenerative medicine and tissue engineering. Preclinical studies have demonstrated that MSCs have the capacity to enhance self-renewal of small intestinal and colonic epithelium<sup>24–27</sup> and accelerate structural recovery after radiation injury.<sup>28,29</sup> A body of evidence shows that the therapeutic benefit of MSCs is induced by the secretion of bioactive molecules.<sup>30,31</sup> MSCs have immunomodulatory properties involving low immunogenicity, the ability to modify the maturation and function of antigen-presenting cells, and an alteration in the cytokine secretion of inflammatory cells. Two experimental studies demonstrated the ability of MSCs to enhance healing after colonic anastomosis.<sup>32,33</sup> Moreover, a previous study showed an improvement in cutaneous blood supply following cutaneous irradiation.<sup>34</sup> Various sources of MSCs have emerged. MSCs from adipose tissue (Ad-MSCs) are abundant, and they are easy to harvest and expand *in vitro*. These properties make Ad-MSCs an autologous cell source that may, in some cases, be valuable for regenerative cell therapy. In this study, we aimed to evaluate the therapeutic benefits of Ad-MSC injections in an experimental rat model of irradiated colonic anastomosis. Mucosal wound healing and inflammatory processes were investigated.

## Materials and Methods

### *Animals, Irradiation, and Sample Collection*

All experiments were performed in compliance with the Guide for the Care and Use of Laboratory Animals as published by the French regulations for animal experiments (Ministry of Agriculture Order No. B92-032-01, 2006) with European Directives (86/609/CEE) and were approved by local ethical committee of the institute of Radioprotection and Nuclear Safety in Fontenay-aux-Roses (P12-04) and Ghent University Hospital (EC: EDC 12/03). Forty-eight Sprague-Dawley (SD) rats (9 wk-old male rats of 300 to 350 g) were purchased from Charles River Laboratories (L'Abresle, France). Rats submitted to RT were anesthetized by isoflurane inhalation, and a single 27 Gray (Gy) dose was delivered by <sup>60</sup>Co source through a 2 × 3 cm window centered on the colorectal region. All rats were marked by ear puncture. On the day of euthanasia, animals were anesthetized by isoflurane inhalation; blood samples were taken under cardiac puncture, and the colon was collected for histological examination and fixed in 4% formaldehyde.

### *Study Design and Administration of Ad-MSCs*

The design of the protocol is described in Fig. 1. The study compared 3 groups that all underwent colonic anastomosis. For group 1, the control/sham group, anastomosis was performed 4 wk after sham irradiation. For group 2, anastomosis was performed 4 wk after irradiation. The same volume of

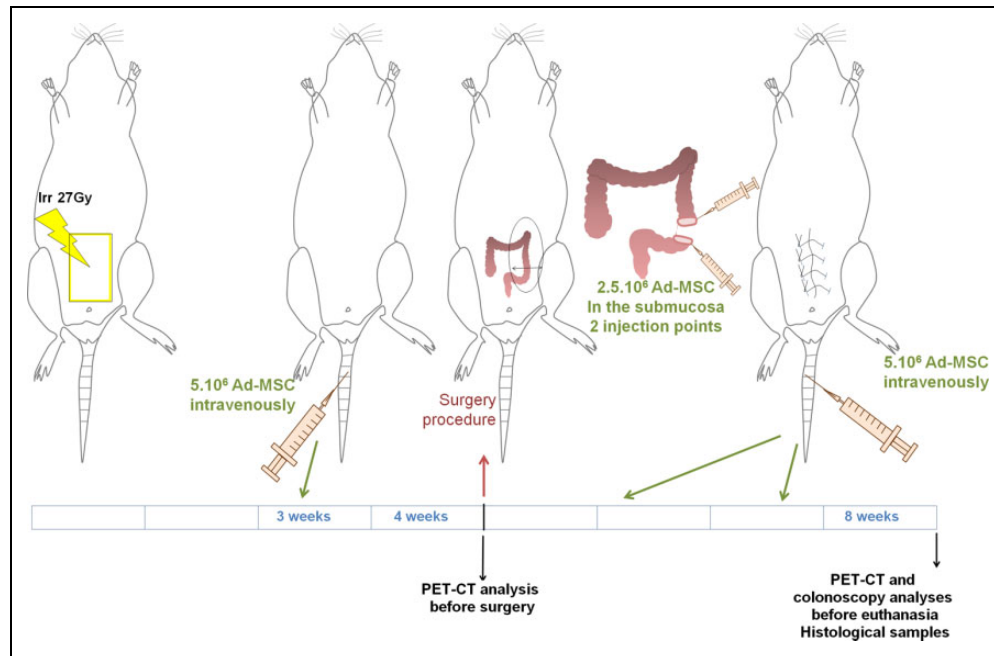


**Figure 1.** Scheme of the experimental procedure. Rats received local irradiation of the colon. Three weeks after irradiation, a first intravenous injection of mesenchymal stromal cells (MSCs) was administered. At 4 wk, before the colonic anastomosis, a positron emission tomography-computed tomography (PET-CT) scan was performed. During the surgical procedure, MSCs were injected locally in the mucosa, after resection, on both sides of the colon. Then, 2 intravenous injections of MSCs were administered (approximately every 10 d). At 8 wk, the rats were submitted to PET-CT scan analyses and colonoscopy. Animals were euthanized, and tissues were collected for histological analyses.

phosphate buffered saline (PBS) 1× was injected at the same time as for group 3 but without Ad-MSCs. Group 3 was irradiated and received Ad-MSC treatment. In this group, 3 wk after radiation exposure,  $5 \times 10^6$  Ad-MSCs in 500  $\mu$ L of PBS 1× were infused into the tail vein. Surgery was performed 1 wk later (i.e., 4 wk after irradiation). During surgery, Ad-MSCs ( $5 \times 10^6$  in 300  $\mu$ L of PBS 1×) were injected locally at 2 injection sites on both edges of the dissected colon before performing anastomosis. Every 10 d, 2 more intravenous injections of  $5 \times 10^6$  Ad-MSCs were performed. During the study, 2  $^{18}\text{F}$ -FDG-PET-CT analyses were performed for each rat (1 d before surgery, i.e., at 4 wk, and 1 d before euthanasia, i.e., at 8 wk). Colonoscopies were performed on all groups before euthanasia (8 wk). All groups were euthanized after 8 wk (study protocol, Fig. 1). For all procedures requiring immobilization, animals were anesthetized by isoflurane inhalation.

### Ad-MSC Culture and Characterization

Subcutaneous inguinal adipose tissue was removed from SD rats, finely minced, and enzymatically digested at 37 °C in minimum essential media (MEM) containing 0.1% collagenase type I (Sigma-Aldrich, St Quentin Fallavier, France) for 30 min (min), 3 times. The digested tissue was filtered through a 100  $\mu$ m filter. Collagenase was then neutralized with culture medium containing 10% fetal bovine serum (FBS). After centrifugation (1200 rpm for 3 min), cells were suspended in MEM $\alpha$  containing 20% FBS, penicillin–

streptomycin and L-glutamin (all from Invitrogen) plated at 1000 cells by  $\text{cm}^2$  and cultured at 37 °C in humidified 5%  $\text{CO}_2$ . After 6 d, the monolayer of adherent cells was trypsinized, washed in PBS 1× 3 times before injection in rats. The phenotype of amplified Ad-MSCs was verified by flow cytometry. The percentage of CD90 (clone OX-7; BD Biosciences) and CD73 (clone 5F/B9; BD Biosciences) positive cells were analyzed, and the absence of hematopoietic cells was verified with CD34 (clone ICO115, Santa Cruz Biotechnology) and CD45 (clone OX-1; BD Biosciences) markers. Isotype identical antibodies served as controls.

### Surgery

Surgery was performed under general inhalation anesthesia induced with 5% isoflurane. The anesthesia was evaluated by reaction on leg pressure and respiration frequency and continued in a steady state with 1.5–2% isoflurane. The rat was fixed in dorsal decubitus under sterile conditions on a heated operation table. The abdomen of the rat was shaved just before surgery and disinfected with povidone iodine. A distal midline laparotomy of 3 to 4 cm was performed. Sharp dissection was used, without electronic or ultrasonic coagulation devices. The distal colon and rectum with the hip as the lowest border were the regions of interest. The cecum and the small bowel were protected and kept out of the operation field with a moist gauze. The abdominal wall and the colon were exposed by 2 traction points. In the irradiated groups, the colon was cut in the center or just above the

irradiated area (white and nonvascularized area). Ad-MSCs or PBS 1× were locally injected at 2 injection sites on both edges of the dissected colon. The anastomosis was realized at 4 cm from the rectum and above the pelvic bone. The colon was sutured end to end with interrupted polydioxanone stitches (PDS® 6/0) with all the knots outside, each 2 mm. The abdomen was closed with polyglactin 910 (Vicryl® 3/0) running suture and the skin with polyglecaprone (Monocryl® 4/0) intracutaneously. Analgesia (Temgesic® 0.03 mg/(mL solution)/kg) was subcutaneously injected.

### Positron Emission Tomography–Computed Tomography ( $^{18}\text{F}$ -FDG-PET-CT)

All animals were food deprived for at least 6 h prior to  $^{18}\text{F}$ -FDG-PET-CT imaging. During the study, 2  $^{18}\text{F}$ -FDG-PET-CT scans were performed in each animal (Fig. 1). Rats were anesthetized with an isoflurane mixture (2–5% isoflurane and medical  $\text{O}_2$ ) to insert a catheter in 1 of the tail veins for intravenous injection of  $19.9 \pm 0.7$  MBq of [ $^{18}\text{F}$ ]FDG (Ghent University Hospital, Nuclear Medicine Department, Belgium) dissolved in 200  $\mu\text{L}$  of saline. Next, the animals were positioned on the heated animal bed of a small animal dedicated PET scanner (FLEX Triumph II; TriFoil Imaging®, Northridge, CA, USA) and 0.8 mL gastrografin was administered rectally, directly followed by a CT scan acquired for coregistration purposes. Animals were placed in the center of the field of view in a prone position, receiving further anesthesia through a nose cone. Body temperature was maintained at  $\sim 37^\circ\text{C}$  by the heated bed. CT projection data were acquired using the following parameters: 256 projections, detector pixel size 50  $\mu\text{m}$ , focal spot size 100  $\mu\text{m}$ , tube voltage 75 kV, tube current 500  $\mu\text{A}$ , and a field of view of 90 mm. Thirty minutes after tracer injection, a 30-min PET scan was acquired in list mode, with a 75-mm axial field of view and a 1.3-mm spatial resolution, on the same scanner and without moving the animal. CT images were analytically reconstructed using a filtered back projection reconstruction algorithm (Cobra Version 7.3.4; Exxim Computing Corporation, Pleasanton, CA, USA) into a  $512 \times 512 \times 512$  matrix with 250  $\mu\text{m}$  isotropic voxel size. The acquired PET images were reconstructed into a  $200 \times 200 \times 64$  matrix by a 2D maximum likelihood expectation maximization algorithm (LabPET Version 1.12.1; TriFoil Imaging) using 50 iterations and a voxel size of  $0.5 \times 0.5 \times 1.175$   $\text{mm}^3$  ( $x$ ,  $y$ ,  $z$ ). Each resultant CT image is inherently coregistered with the corresponding PET scan. PET and CT images were imported into a medical image data examiner and volumes of interest, determined on sagittal, coronal, and transversal reconstructed CT slices, were drawn over the colon to quantify the uptake of [ $^{18}\text{F}$ ]FDG in the colon, expressed in MBq/mL.<sup>35</sup>

### Endoscopy and Scoring Methods

Colonoscopic analyses were performed at 8 wk after RT on anesthetized rats with a pediatric bronchoscope (Pentax,

France, Argenteuil). Colonic anastomotic healing was observed and scored as described in Supplemental Fig. 1.

### Histological Analyses and Healing Assessment Method

Colon specimens were embedded in paraffin, cut into 5  $\mu\text{m}$  sections, and stained with hematoxylin–eosin–safran. Histological sections of normal colon showed organized and aligned crypts. In the irradiated and operated segment, 2 areas were identified: an ulcerated area without any crypts and a dystrophic area composed of atypical crypts. The size of each area was measured as designed in Fig. 2A, using Histolab software, v10.6.0 (MicroVision Inc., Redmond, WA, USA).

### Immunostaining Analyses

For immunohistochemistry analyses of vessels, sections were dewaxed then placed in an antigen retrieval solution (0.01 M citrate buffer, pH = 6 [DakoCytomation, Trappes, France] for  $3 \times 5$  min at 350 W). The endogenous peroxidases were inhibited by incubation with 3%  $\text{H}_2\text{O}_2$  in methanol at room temperature (RT) for 10 min. After saturation (X0909; DakoCytomation), rabbit antirat von Willebrand factor (vWF) diluted at 350e (Abcam, Paris, France) was applied to the section for 1 h at  $37^\circ\text{C}$ . Staining was developed with Histogreen substrate (E109; Abcys), and sections were counterstained with nuclear fast red (S1963; DakoCytomation, Trappes, France), dehydrated and mounted. Isotype control antibodies are used as negative controls. The number of vascular sections (vWF positive) was numbered on defined surface using a Leica microscope (Nanterre, France) and Histolab software (MicroVision Inc.,). For CD68 and CD163 coimmunostaining (macrophage analyses), tissue sections were treated with proteinase K (DakoCytomation) at RT for 5 min and quenched for endogenous peroxidases as described above. After saturation, mouse antirat CD68 (AbD Serotec, Biorad, Marnes-la-coquette, France) or mouse antirat CD163 (AbDserotec, Peterborough, UK) was applied to the section for 1 h at  $37^\circ\text{C}$ . Tissue sections were incubated with goat antimouse Alexa fluor 568 (Invitrogen) and with donkey antimouse Alexa fluor 488 (Invitrogen), respectively, for 30 min at RT. The tissue sections were mounted with Vectashield hard-set (Vector Laboratories) and visualized under a fluorescence confocal microscope (LSM 780; Carl Zeiss, Jena, Germany). The double staining was evaluated using Zen® software, version 2012.

### Statistical Analyses

All data are presented as mean  $\pm$  standard error of mean. Statistical analyses were performed using Sigma plot V11.0 (Systat Software, Erkrath, Germany). Differences between groups were analyzed using the unpaired student  $t$  test or nonparametric Mann–Whitney test when necessary.  $P < 0.05$  was considered to indicate statistical significance.

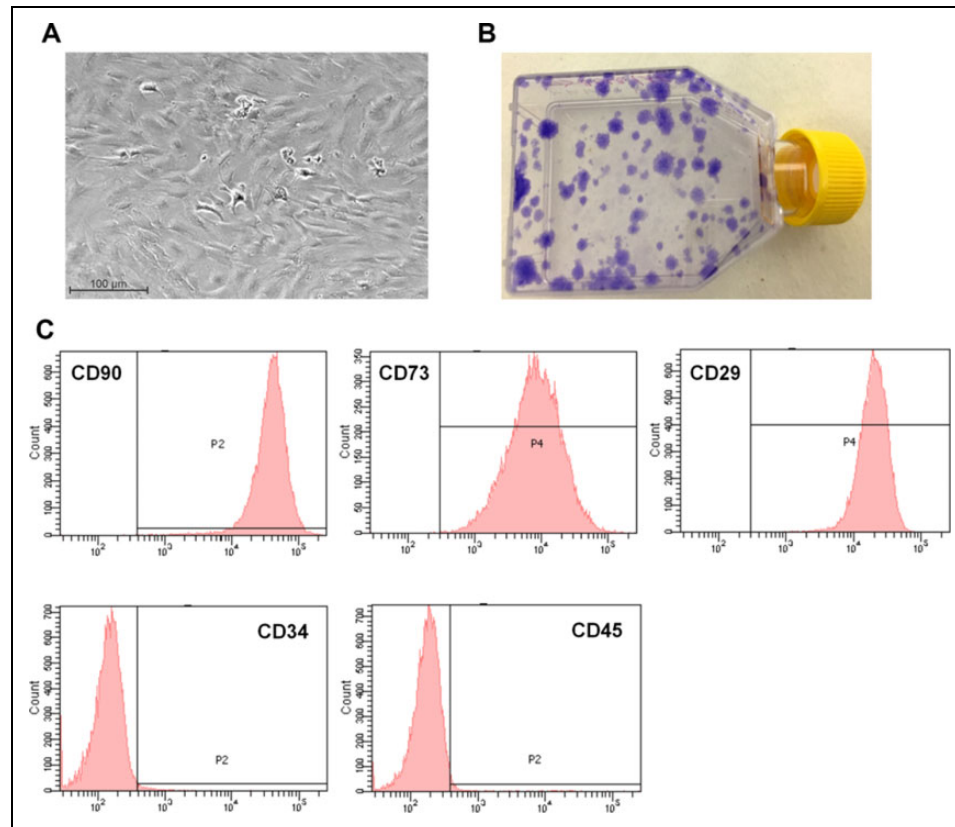


**Figure 2.** Characterization of MSCs before injection. (a) Morphology of the Ad-MSCs in culture before injection (b) Representative picture of colony-forming unit-fibroblast (CFU-F) assay stained with crystal violet. The CFU-F assay has been used to enumerate the number of Ad-MSCs within the initial cell preparation. (c) Flow cytometry analysis of MSCs before injection. MSCs expressed high levels of CD90, CD73 and CD29 specific markers (upper panel). MSCs did not express hematopoietic marker as CD34 and CD45 (lower panel).

## Results

### Ad-MSC Phenotype and Differentiation

Cells isolated from adipose tissue were plated under specific culture conditions. They exhibited homogenous spindle-shaped morphology (Fig. 3A). The capacity to form colony-forming units was evaluated: there were  $62.06 (\pm 4.46)$  for 1000 cells seeded in  $25 \text{ cm}^2$  (Fig. 3B). The Ad-MSC phenotype was analyzed for stromal characteristics by flow cytometry at passages 0 and 1. The cells expressed high levels of CD90, CD73, and CD29, and they were negative for hematopoietic markers (Fig. 3C). On average, Ad-MSCs expressed CD90 at 96.6% ( $\pm 0.19\%$ ), CD73 at 100%, CD29 at 100%, CD34 at 0.1% ( $\pm 0.06\%$ ), and CD45 at 0.5% ( $\pm 0.19\%$ ).

### General Results

The study was divided into 4 series of 3 groups of rats: sham (group 1, or G1), irradiated (G2), and both irradiated and treated with Ad-MSCs (G3). In the first 2 series, almost all the irradiated rats died, whether they were treated with Ad-MSCs (8 of 8) or not (7 of 8). Deaths always occurred 5 to 10 d after surgery. All rats of the sham groups survived (7 of 7). We

concluded that the surgical technique alone was not the problem, but rather the combination of surgery and irradiation. Perioperative examination and autopsy showed that the level of irradiation was too low in the pelvis, leading to traction during surgery and tissue tearing. All autopsies revealed no perforation but extensive in a frozen pelvis. In the subsequent 2 series, the field of radiation was applied more proximally to the colon, and the colon was cut immediately above the irradiated area (G1,  $n = 4$ ; G2 and G3,  $n = 10$ ). This change in technique improved survival in the irradiated groups (Fig. 4A). In terms of weight changes, no significant difference was observed between the irradiated groups (Fig. 4B).

### Macroscopic Evaluation of Ad-MSC Treatment for Colonic Anastomosis After Irradiation

Before euthanasia, colonic damage was evaluated using endoscopy (Fig. 5A). Details on scoring (Fig. 5B) are given in Supplemental Figure 1. In G1 (sham), we observed complete healing following colonic anastomosis, together with a great number of vessels. In G2 (irradiated), colonic anastomosis was associated with a large amount of necrotic tissue and fibrin, as revealed by white and brown deposits. In G3

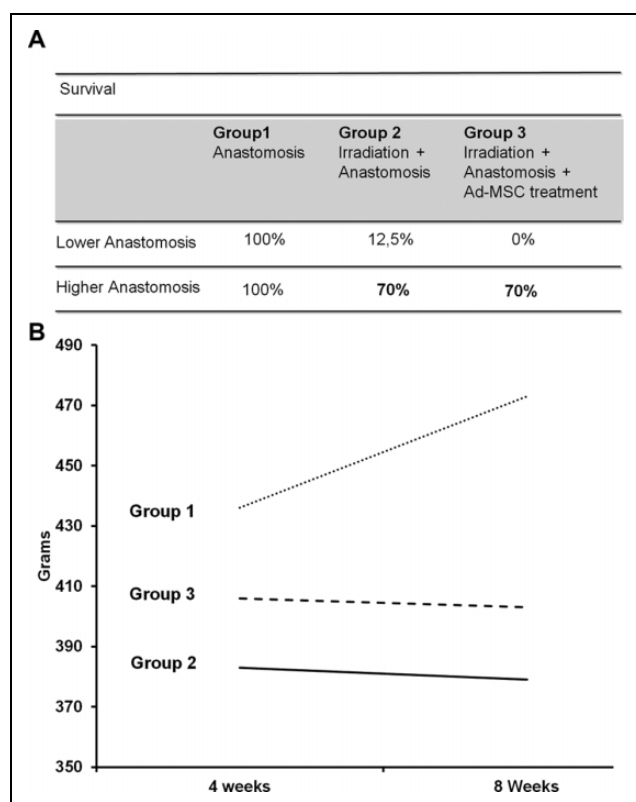


**Figure 3.** (A) Rat survival according to localization of the colonic anastomosis. For lower anastomosis,  $n = 8$  animals for each group. For higher anastomosis,  $n = 4$  animals for group 1 and  $n = 10$  animals for groups 2 and 3. (B) Body weight of animals was monitored at 4 and 8 wk ( $n = 4$  animals for group 1 and  $n = 10$  animals for groups 2 and 3).

(irradiated and treated with Ad-MSCs), we observed fewer necrotic patches around the anastomosis than in G2. However, the treatment did not allow complete healing, which was observed in G1. We also evaluated the amount of bleeding during colonoscopy (Fig. 5B). After irradiation and surgery, colonoscopy triggered hemorrhaging in >57% of all rats. In G1, however, bleeding was found in only 1 (14.3%) rat.

### Assessment of Ad-MSC Therapeutic Benefit on Colonic Healing Using Histological Criteria

The rats were sacrificed 8 wk postirradiation, and anastomotic healing was assessed by measuring the size of the colonic scar (i.e., area without crypt and ulcer) and atypical mucosa (i.e., area with disorganized crypts; Fig. 2A). We observed that the size of the atypical area was not modified, regardless of whether rats were administered Ad-MSC treatment. However, the ulcerated area was statistically smaller after treatment with Ad-MSCs ( $P < 0.05$ ; Fig. 2B).

We also counted, on histological slides, vascular sections of the anastomosis for each group of animals. Irradiation (G2 and G3) reduced the number of vascular sections compared to the sham treatment (G1). Furthermore, the number of

vascular sections was normalized in animals that received Ad-MSC treatment (Fig. 2C).

### Analyses of Inflammatory Process Using Noninvasive PET/CT and Immunohistochemistry

Radioactive tracer was injected intravenously, and 30 min later images were acquired by PET scan (Fig. 6A), CT images were analyzed, and results were expressed as means in Becquerels (Bq; Fig. 6B). In G1, PET scans were performed before the surgery, determining the basal metabolic level (control). Inflammatory response in G1 4 wk after colonic anastomosis (i.e., at 8 wk), the metabolic activity was not significantly increased; thus, no substantial inflammatory response could be attributed to anastomosis 4 wk after the operation. However, in the irradiated group, 4 wk after colonic irradiation (before surgery), the mean of metabolic activity was increased by 65% compared to G1. The study design allowed us to consider the effect of 1 intravenous Ad-MSC injection on the inflammatory process 4 wk after irradiation. The results demonstrated that inflammation in G2 was significantly greater than in G1 ( $P = 0.03$ ), whereas greater inflammation in G3 was not significant ( $P = 0.16$ ). We noted that Ad-MSCs induced a 21.1% reduction in inflammation 7 d after treatment. However, the lower degree of inflammation observed in G3 with respect to G2 at 8 wk, measured as means in Becquerels, was not significant.

To extend our analysis of the therapeutic effects of Ad-MSCs on the inflammatory process, we studied macrophage infiltrates on histological slides, 8 wk after irradiation. Macrophage subpopulations are addressed in the literature, and the M2 subpopulation in particular has been described as a key player in the wound healing process.<sup>36</sup> Using double immunolabeling (CD163 and CD68), we determined M2 proportions for the different groups (Fig. 7). In G1, we found few M2 macrophages in the colonic lamina propria. As expected, after irradiation and surgery (G2), the total number of macrophages greatly increased. In G3, the proportion of M2 macrophages (CD163CD68 costaining) in the total CD68-stained cell population was 49.3%. The M2 percentage had risen (Fig. 7).

### Discussion

Anastomotic dehiscence is one of the most serious potential complications of colorectal surgery. An understanding of the normal healing process for wounds, in general, and surgical wounds or anastomoses, in particular, is essential for the treatment of anastomotic leakage. Although such healing has long been studied, it is still not completely understood. Described in phases defined according to time elapsed since injury,<sup>37</sup> it is a dynamic, interactive process involving blood cells, parenchymal cells, soluble mediators, and the extracellular matrix. The first phase is *hemostasis*. This starts immediately and is characterized by vasoconstriction, initiation of the coagulation cascade, and platelet activation,<sup>38</sup> and resulting in a fibrin/fibronectin matrix that temporarily seals and connects the 2



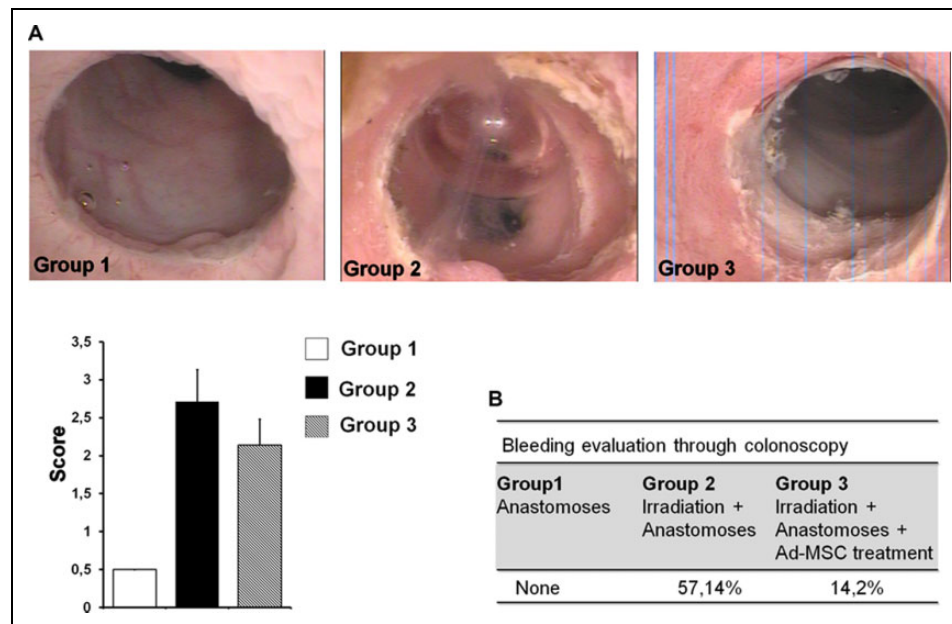


**Figure 4.** (A) Representative pictures of colonoscopy analysis of each group and graph of the score obtained for  $n = 7$  animals in each group. (B) Table of evaluation of bleeding in each group during the colonoscopy (8 wk).

bowel ends. The *inflammatory phase* is next: vessels dilate and become more permeable. Phagocytosis of damaged tissue involves neutrophils first and macrophages later.<sup>39</sup> Both cell types produce inflammatory cytokines, including tumor necrosis factor  $\alpha$  (TNF- $\alpha$ ), interleukin 1 (IL-1), and proteases. Macrophages also secrete transforming growth factor  $\beta$  (TGF $\beta$ ), TGF $\alpha$ , and platelet-derived growth factor (PDGF), modulating fibroblast activity as well as the inflammatory response, reepithelialization, and angiogenesis. They thus play an important role in wound healing. The *proliferative phase*, which overlaps with the inflammatory phase, involves deposition of collagen and formation of new extracellular matrix. At the same time, angiogenesis is initiated when tissues secrete vascular endothelial growth factor (VEGF), which directly triggers the proliferation of endothelial and smooth muscle cells. The mucosa is also regenerated by epithelial cell hyperplasia and migration. During the final remodeling or *maturation phase*, collagen homeostasis is achieved and marked by changes in types of collagen as well as an increase in tensile strength through cross-linking of collagen fibers.

As the colon harbors the densest bacterial population, operative procedures involving resection and anastomosis of the colon are associated with higher rates of surgical site infection or leakage. Several risk factors for anastomotic leakage have been identified. They include certain patient profiles and the use of neoadjuvant RT as well as particular drugs, like steroids. Several studies on sealing or reinforcement have been completed or are ongoing. Fibrin glue has no effect, and other tissue adhesives or pharmacological interventions are not effective or need further investigations.<sup>9,13,40–43</sup> The persistence of foreign antigens or dense bacterial colonization of the wound site can lead to

a prolonged inflammatory response. This is marked by the continued presence of innate immune cells releasing high amounts of protease and reactive oxygen species that may also damage the extracellular matrix. The use of preventive systemic antibiotics perioperatively has become a standard of care.<sup>44</sup> Mechanical bowel preparation continues to be a controversial subject. When followed by treatment with appropriate oral antibiotics, it has been reported to reduce surgical site infections.<sup>45</sup> The healing process thus described inevitably depends on adequate vascular supply and oxygenation. Ischemia in tissue surrounding the site of anastomosis is one cause of anastomotic leakage having a major impact on wound healing. Though chemical agents have been introduced, in particular a molecule that enhances vasodilatation by smooth muscle relaxation in the vessels, observed effects have not been promising.<sup>32,46</sup>

Stem cell research has received much attention in recent years and their use has been shown to have beneficial effects. Many studies have focused on MSCs from bone marrow or adipose tissue, since they can easily be undifferentiated/amplified in vitro, they are immunocompatible, and their use is not ethically controversial. These MSCs represent a novel means of repairing injured tissue through their proregenerative, proangiogenic, and anti-inflammatory activity. Furthermore, therapeutic benefits for intestinal damage induced by radiation or inflammation have been reported.<sup>28</sup> Experiments performed on animal models with colorectal damage similar to that observed in patients developing severe side effects after RT have shown that MSC treatment yields better epithelial injury scores and limits fibrosis.<sup>47,48</sup> In one model of sutured gastric perforation, injection of MSCs favored wound healing<sup>49</sup>; however, no report showing

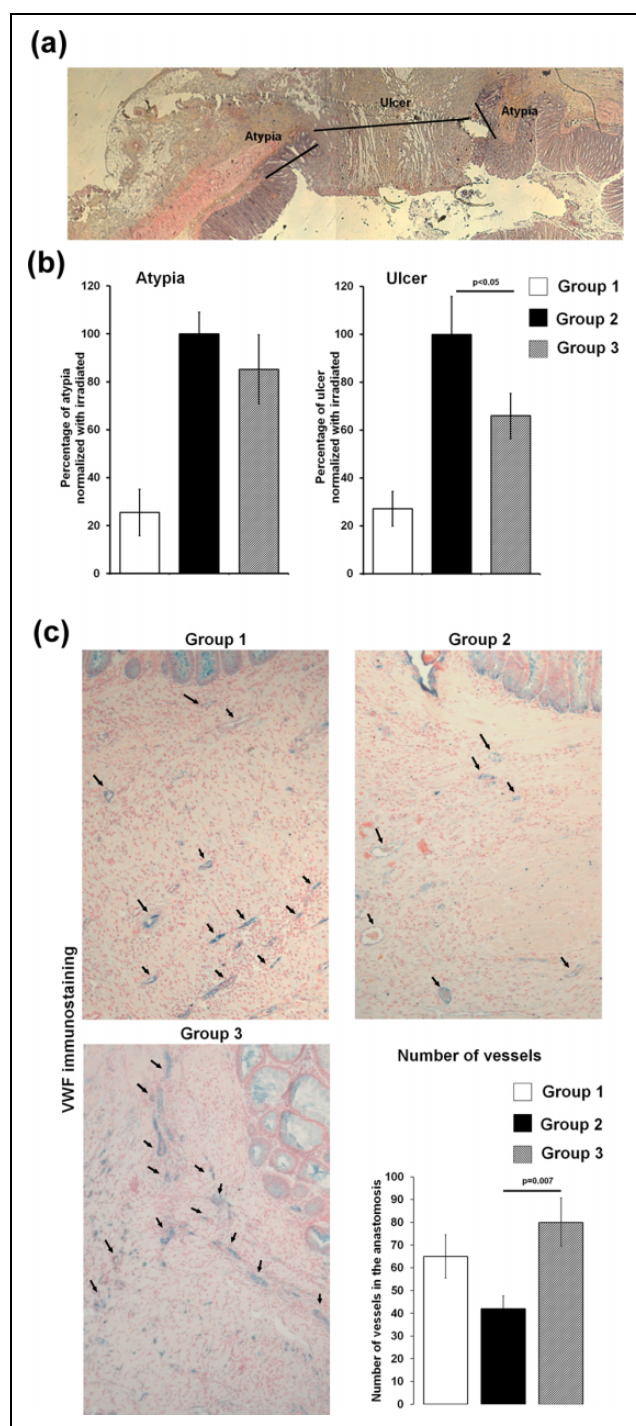


**Figure 5.** (A) Representative histologic slides of colonic anastomosis after irradiation stained with hematoxylin–eosin–safran (HES). The size of the atypia and ulcer was measured as mentioned by arrows on the picture. (B) Graph of mean atypia and ulcer size normalized with irradiation of each experiment (8 wk). For each group,  $n = 7$  animals; statistical analysis of group 2 versus group 3 was carried out using Mann-Whitney test. (C) Analyses of vascularization process on histologic slides at 8 wk. Representative pictures of von Willebrand factor immunostaining (blue) and nuclear fast red counterstaining (pink). The numbers of vessels were counted using Histolab software, and results were report on the graph ( $\pm$  standard error of the mean [SEM]). For each group,  $n = 7$  animals; statistical analysis of group 2 versus group 3 was carried out using t test.

enhanced healing following colonic anastomosis and irradiation has been published. In this study, iterative Ad-MSC treatment (3 injections) statistically reduced the size of the ulcer scar measured on histological slides. Decreased hemorrhaging after colonoscopy was also observed. Similarly, pre-clinical and clinical data have revealed that after severe radiation damage, repeated injections of MSCs are needed to improve wound healing.<sup>5,48</sup> The substantial therapeutic effects of MSCs may be attributed to the wide range of substances they secrete.<sup>30</sup> In previous studies, we demonstrated that MSCs from bone marrow stimulate proliferation of epithelial cells in colonic crypts near the ulcer, leading to reduction in mucosal damage.<sup>47</sup> Few MSCs were detected in the damaged area, suggesting a therapeutic effect through systemic action, probably induced by MSCs trapped in the lung, as suggested by Prockop et al.<sup>50</sup> In this study, although some Ad-MSCs were locally injected, they were not detected in the irradiated colon after anastomosis (data not provided). As in our previous study, we believe that therapeutic benefit is probably mediated by the stimulation of the secretion of molecules by endogenous cells that enhance the endogenous regenerative process.

Neovascularization permits tissue perfusion and oxygenation, thereby playing a very important role in anastomotic healing. However, irradiation leads to endothelial cell apoptosis, increased vascular dilatation and permeability, and acquisition of a pro-inflammatory and procoagulant phenotype.<sup>51</sup> These modifications strongly contribute to the development and chronicity of radiation-induced injury. In this study, we observed major bleeding after colonoscope insertion in irradiated rats. This suggests that irradiation modifies vessel structure. We also noted that, in irradiated and operated colons, the number of vascular sections after 8 wk was lower than in sham animals (G1). However, after Ad-MSC treatment, the number of vascular sections is comparable to that in sham animals. Histological data demonstrated that vessels detected are small, which may suggest induction of neovascularization. In the small intestine, it has already been demonstrated that MSCs induce the formation of a large number of microvessels associated with an increase in *VEGF* gene expression.<sup>52</sup> Together these results suggest an improvement of the vascular compartment and greater quality and number of vessels after cell therapy. A better vascular network may enhance the intake of growth factors and nutrients, thus favoring the proregenerative process. However, the Ad-MSC treatment did not induce complete epithelial healing of colonic anastomosis as observed in nonirradiated rats. This may be due to the animal model employed. This study applied a single high dose of irradiation (29 Gy) to the rat bowel.<sup>47</sup> This likely has a major effect on most cells in the target area, resulting in a substantial loss of regenerative potential and tissue integrity. In contrast, in patients undergoing fractionated irradiation, some multipotent but quiescent cells in the crypt may survive irradiation and be available for tissue regeneration. Indeed, a large body of data demonstrates that Ad-MSCs stimulate



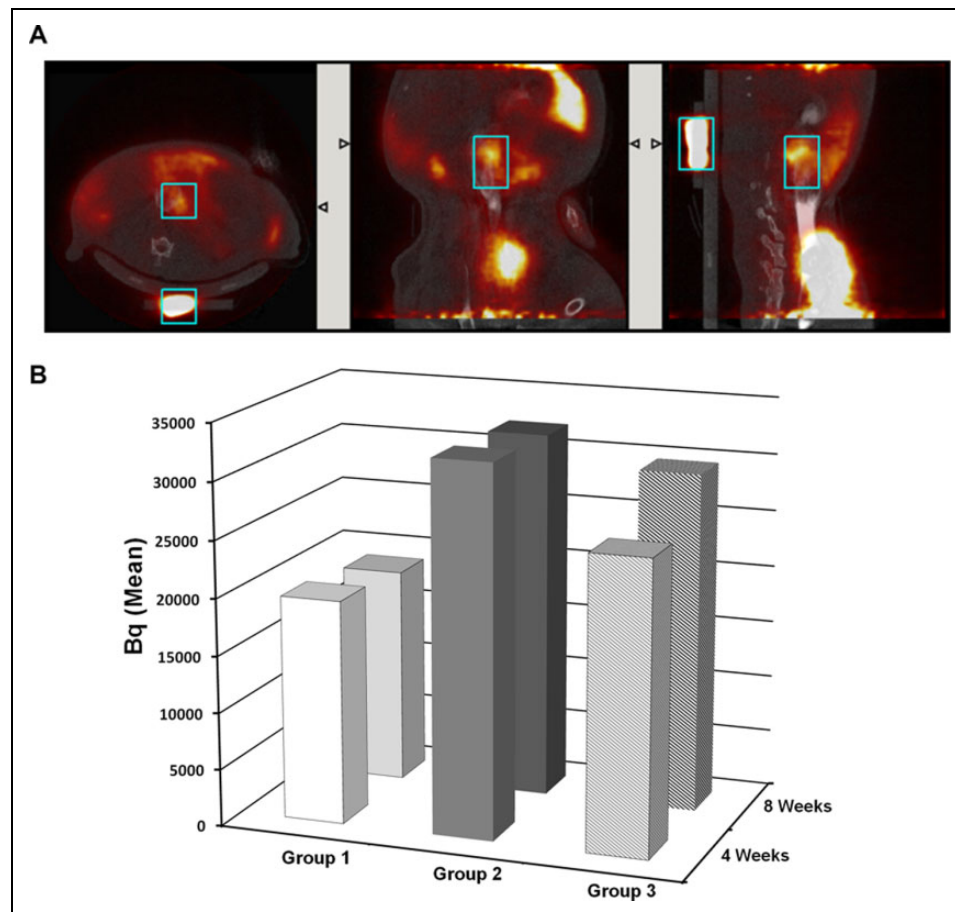


**Figure 6.** (A) Representative images obtained with positron emission tomography–computed tomography (PET-CT) scan after intravenous injection of a radioactive [ $^{18}\text{F}$ ]FDG tracer according to sagittal section (left panel), coronal section (middle panel), and transversal section (right panel). The window of interest was designed, and the intensity of the signal (in Becquerel) was measured. (B) Graph of mean ( $\pm$  standard error of the mean) Becquerel obtained in each groups at 4 and 8 wk. Statistics (4 wk) group 1 versus group 2,  $*P = 0.03$ ; group 1 versus group 3,  $P = 0.16$ . Group 1: 4 wk;  $n = 7$ ; 8 wk;  $n = 11$ . Group 2: 4 wk;  $n = 18$ ; 8 wk;  $n = 8$ . Group 3: 4 wk;  $n = 17$ ; 8 wk;  $n = 7$ .

host endogenous tissue regeneration, offering greater therapeutic benefit in regenerative animal models. Thus, it is possible that our study employed an extreme animal model and that Ad-MSCs would have been more therapeutic after fractionated irradiation. In previous laboratory studies, fractionated doses of irradiation (52 Gy in 4-Gy increments) did not induce epithelial damage<sup>53</sup> as observed in patients treated for rectal adenocarcinoma.<sup>47</sup> In this study, the irradiation protocol-induced histological damage similar to that observed in patients suffering severe side effects after pelvic RT; it thus offers an appropriate animal model.<sup>47</sup> The results obtained are a first step toward limiting irreversible ulceration after irradiation and colonic anastomosis.

The inflammatory process is essential to the initiation of wound healing. However, it has been shown that persistent inflammation is a feasible predictor of elevated risk of colon anastomotic leakage.<sup>36</sup> In this study, we used  $^{18}\text{F}$ -FDG-PET/CT analysis to quantify inflammation. In irradiated animals, we found that at the time of surgery (4 wk after irradiation), the metabolic activity is in high

gear. However, in the group of rats that received 1 intravenous injection of Ad-MSCs, the inflammatory process was more limited in extent, though this effect was not observed at 8 wk. Analysis of macrophage infiltrates revealed that after Ad-MSC treatment, the proportion of M2 macrophages grew. It has already been demonstrated that the prevention of colorectal anastomotic leakage is associated with the presence of anti-inflammatory M2 macrophages.<sup>36</sup> Taken as a whole, these findings suggest that Ad-MSC treatment modifies the inflammatory process, favoring the M2 phenotype and promoting wound healing.

In conclusion, cell therapy using MSCs from adipose tissue impedes radiation-induced injury and improves colonic anastomotic healing after irradiation by enhanced vascular supply and reduced inflammation. These results suggest a possible role in the clinical prevention and treatment of radiation-induced rectocolitis and anastomotic healing in patients undergoing neoadjuvant RT. This study demonstrates that MSC treatment has multitargeted effects<sup>52</sup> that could promote colonic anastomotic

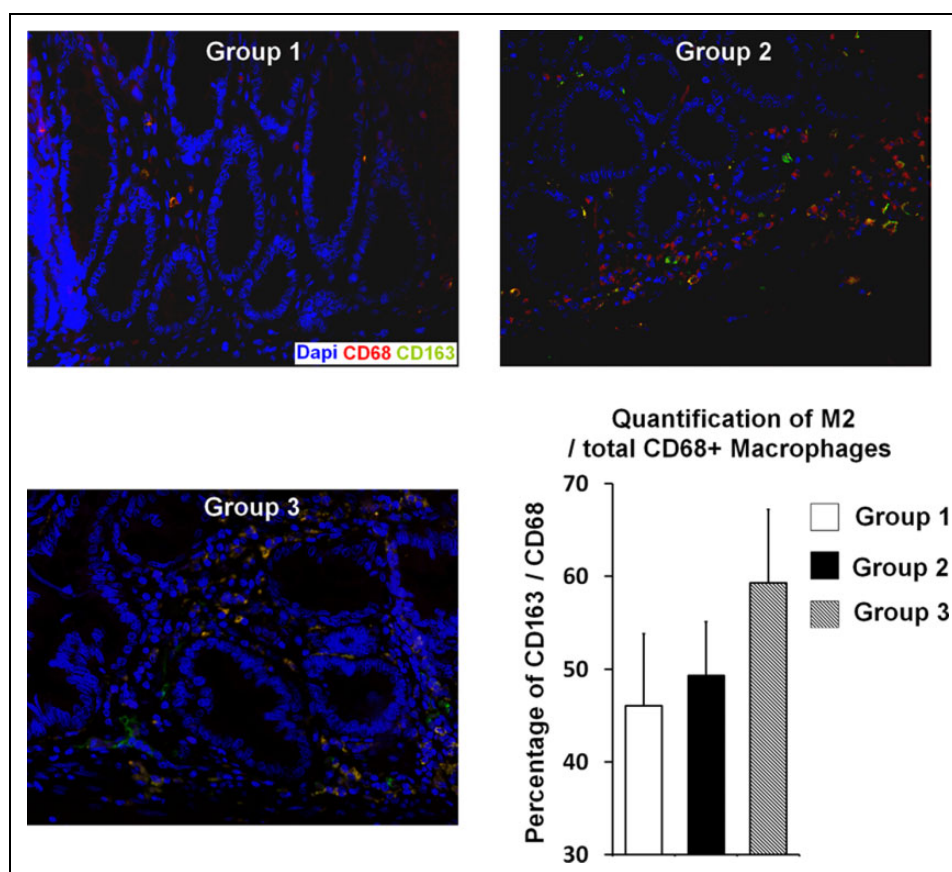


**Figure 7.** (A) Analyses of type 2 macrophage (M2) infiltrate in each group (8 wk). Representative picture of double immunostaining using CD68 antibody (red) shows total macrophages and CD163 antibody (green) counterstained with 4',6-diamidino-2-phenylindole (DAPI; blue). Quantification of M2 macrophages (yellow merging signal) was realized using Zen software, version 2012. The percentage of M2 among the CD68-positive population was reported on the graph. Group 1  $n = 4$ , group 2  $n = 5$ , and group 3  $n = 3$  at 8 wk.

healing after irradiation. Though future developments, such as shielding of injected cells in the irradiated area,<sup>54</sup> may further enhance therapeutic effects, these results are encouraging for the use of MSCs in regenerative medicine.

### Acknowledgments

We are grateful to Inge Vandenbroucke, Saskia De Groote, Benedicte Descamps, Natascha Rosseel, Alexandra Sémont for their help and advice. Lara Moussa is supported by the French “Agence Nationale pour la Recherche” 13-RPIB-0008-ANTHOS. Wim Cee-len is a senior clinical investigator from the Fund for Scientific Research—Flanders (FWO)

### Ethical Approval

Experiments approved by the local ethical committee of the institute of Radioprotection and Nuclear Safety in Fontenay-aux-Roses (P12-04) and Ghent University Hospital (EC: EDC 12/03).

### Statement of Human and Animal Rights

All experiments were performed in compliance with the Guide for the Care and Use of Laboratory Animals; rats were anesthetized by isoflurane inhalation.

### Statement of Informed Consent

There are no human subjects in this article and informed consent is not applicable.

### Declaration of Conflicting Interests

The author(s) declared no potential conflicts of interest with respect to the research, authorship, and/or publication of this article.

### Funding

The author(s) received no financial support for the research, authorship, and/or publication of this article.

### Supplemental material

Supplementary material is available for this article online.

### References

1. Hauer-Jensen M, Denham JW, Andreyev HJ. Radiation enteropathy—pathogenesis, treatment and prevention. *Nat Rev Gastroenterol Hepatol*. 2014;11(8):470–479.
2. Kapiteijn E, Marijnen CA, Nagtegaal ID, Putter H, Steup WH, Wiggers T, Rutten HJ, Pahlman L, Glimelius B, van Krieken JH, et al; Dutch Colorectal Cancer Group. Preoperative

- radiotherapy combined with total mesorectal excision for resectable rectal cancer. *N Engl J Med*. 2001;345(9):638–646.
3. Frykholm GJ, Glimelius B, Pahlman L. Preoperative or postoperative irradiation in adenocarcinoma of the rectum: final treatment results of a randomized trial and an evaluation of late secondary effects. *Dis Colon Rectum*. 1993;36(6):564–572.
4. Ward MC, Tendulkar RD, Ciezki JP, Klein EA. Future directions from past experience: a century of prostate radiotherapy. *Clin Genitourin Cancer*. 2014;12(1):13–20.
5. Lataillade JJ, Doucet C, Bey E, Carsin H, Huet C, Clairand I, Bottollier-Depois JF, Chapel A, Ernou I, Gourven M, et al. New approach to radiation burn treatment by dosimetry-guided surgery combined with autologous mesenchymal stem cell therapy. *Regen Med*. 2007;2(5):785–794.
6. Hauer-Jensen M, Wang J, Denham JW. Bowel injury: current and evolving management strategies. *Semin Radiat Oncol*. 2003;13(3):357–371.
7. Juloori A, Tucker SL, Komaki R, Liao Z, Correa AM, Swisher SG, Hofstetter WL, Lin SH. Influence of preoperative radiation field on postoperative leak rates in esophageal cancer patients after trimodality therapy. *J Thorac Oncol*. 2014;9(4):534–540.
8. Van Daele E, Van de Putte D, Ceelen W, Van Nieuwenhove Y, Pattyn P. Risk factors and consequences of anastomotic leakage after Ivor Lewis oesophagectomy dagger. *Interact Cardiovasc Thorac Surg*. 2016;22(1):32–37.
9. Pommergaard HC, Gessler B, Burcharth J, Angenete E, Haglund E, Rosenberg J. Preoperative risk factors for anastomotic leakage after resection for colorectal cancer: a systematic review and meta-analysis. *Colorectal Dis*. 2014;16(9):662–671.
10. Nisar PJ, Lavery IC, Kiran RP. Influence of neoadjuvant radiotherapy on anastomotic leak after restorative resection for rectal cancer. *J Gastrointest Surg*. 2012;16(9):1750–1757.
11. Eriksen MT, Wibe A, Norstein J, Haffner J, Wiig JN. Anastomotic leakage following routine mesorectal excision for rectal cancer in a national cohort of patients. *Colorectal Dis*. 2005;7(1):51–57.
12. Shekarriz H, Eigenwald J, Shekarriz B, Upadhyay J, Shekarriz J, Zoubie D, Wedel T, Wittenburg H. Anastomotic leak in colorectal surgery: are 75% preventable? *Int J Colorectal Dis*. 2015;30(11):1525–1531.
13. Oines MN, Krarup PM, Jorgensen LN, Agren MS. Pharmacological interventions for improved colonic anastomotic healing: a meta-analysis. *World J Gastroenterol*. 2014;20(35):12637–12648.
14. McDermott FD, Heeney A, Kelly ME, Steele RJ, Carlson GL, Winter DC. Systematic review of preoperative, intraoperative and postoperative risk factors for colorectal anastomotic leaks. *Br J Surg*. 2015;102(5):462–479.
15. Theis VS, Sripadam R, Ramani V, Lal S. Chronic radiation enteritis. *Clin Oncol (R Coll Radiol)*. 2010;22(1):70–83.
16. Moussa L, Usunier B, Demarquay C, Benderitter M, Tamarat R, Semont A, Mathieu N. Bowel radiation injury: complexity of the pathophysiology and promises of cell and tissue engineering. *Cell Transplant*. 2016;25(10):1723–1746.
17. Faiella W, Atoui R. Therapeutic use of stem cells for cardiovascular disease. *Clin Transl Med*. 2016;5(1):34.
18. Liu Y, Tang SC. Recent progress in stem cell therapy for diabetic nephropathy. *Kidney Dis (Basel)*. 2016;2(1):20–27.
19. Maxson S, Lopez EA, Yoo D, Danilkovitch-Miagkova A, Leroux MA. Concise review: role of mesenchymal stem cells in wound repair. *Stem Cells Transl Med*. 2012;1(2):142–149.
20. Wang Q, Duan F, Wang MX, Wang XD, Liu P, Ma LZ. Effect of stem cell-based therapy for ischemic stroke treatment: a meta-analysis. *Clin Neurol Neurosurg*. 2016;146:1–11.
21. Savukinas UB, Enes SR, Sjolund AA, Westergren-Thorsson G. Concise review: the bystander effect: mesenchymal stem cell-mediated lung repair. *Stem Cells*. 2016;34(6):1437–1444.
22. Stoltz JF, de Isla N, Li YP, Bensoussan D, Zhang L, Huselstein C, Chen Y, Decot V, Magdalou J, Li N, et al. Stem cells and regenerative medicine: myth or reality of the 21th century. *Stem Cells Int*. 2015;2015:734731.
23. Brooke G, Cook M, Blair C, Han R, Heazlewood C, Jones B, Kambouris M, Kollar K, McTaggart S, Pelekanos R, et al. Therapeutic applications of mesenchymal stromal cells. *Semin Cell Dev Biol*. 2007;18(6):846–858.
24. Bessout R, Semont A, Demarquay C, Charcosset A, Benderitter M, Mathieu N. Mesenchymal stem cell therapy induces glucocorticoid synthesis in colonic mucosa and suppresses radiation-activated T cells: new insights into MSC immunomodulation. *Mucosal Immunol*. 2014;7(3):656–669.
25. Semont A, Francois S, Mouiseddine M, Francois A, Sache A, Frick J, Thierry D, Chapel A. Mesenchymal stem cells increase self-renewal of small intestinal epithelium and accelerate structural recovery after radiation injury. *Adv Exp Med Biol*. 2006;585:19–30.
26. Semont A, Mouiseddine M, Francois A, Demarquay C, Mathieu N, Chapel A, Sache A, Thierry D, Laloi P, Gourmelon P. Mesenchymal stem cells improve small intestinal integrity through regulation of endogenous epithelial cell homeostasis. *Cell Death Differ*. 2010;17(6):952–961.
27. Thomas ED. A history of haemopoietic cell transplantation. *Br J Haematol*. 1999;105(2):330–339.
28. Chang PY, Qu YQ, Wang J, Dong LH. The potential of mesenchymal stem cells in the management of radiation enteropathy. *Cell Death Dis*. 2015;6:e1840.
29. Chapel A, Francois S, Douay L, Benderitter M, Voswinkel J. New insights for pelvic radiation disease treatment: multipotent stromal cell is a promise mainstay treatment for the restoration of abdominopelvic severe chronic damages induced by radiotherapy. *World J Stem Cells*. 2013;5(4):106–111.
30. Caplan AI. Adult mesenchymal stem cells: when, where, and how. *Stem Cells Int*. 2015;2015:628767.
31. Meirelles Lda S, Fontes AM, Covas DT, Caplan AI. Mechanisms involved in the therapeutic properties of mesenchymal stem cells. *Cytokine Growth Factor Rev*. 2009;20(5–6):419–427.
32. Adas G, Arikan S, Karatepe O, Kemik O, Ayhan S, Karaoz E, Kamali G, Eryasar B, Ustek D. Mesenchymal stem cells improve the healing of ischemic colonic anastomoses

- (experimental study). *Langenbecks Arch Surg*. 2011;396(1):115–126.
33. Yoo JH, Shin JH, An MS, Ha TK, Kim KH, Bae KB, Kim TH, Choi CS, Hong KH, Kim J, et al. Adipose-tissue-derived stem cells enhance the healing of ischemic colonic anastomoses: an experimental study in rats. *J Korean Soc Coloproctol*. 2012;28(3):132–139.
34. Ebrahimian TG, Pouzoulet F, Squiban C, Buard V, Andre M, Cousin B, Gourmelon P, Benderitter M, Casteilla L, Tamarat R. Cell therapy based on adipose tissue-derived stromal cells promotes physiological and pathological wound healing. *Arterioscler Thromb Vasc Biol*. 2009;29(4):503–510.
35. Loening AM, Gambhir SS. AMIDE: a free software tool for multimodality medical image analysis. *Mol Imaging*. 2003;2(3):131–137.
36. Wu Z, Vakalopoulos KA, Boersema GS, Kroese LF, Lam KH, van der Horst PH, Mulder IM, Bastiaansen-Jenniskens YM, Kleinrensink GJ, Jeekel J, et al. The prevention of colorectal anastomotic leakage with tissue adhesives in a contaminated environment is associated with the presence of anti-inflammatory macrophages. *Int J Colorectal Dis*. 2014;29(12):1507–1516.
37. Lundy JB. A primer on wound healing in colorectal surgery in the age of bioprosthetic materials. *Clin Colon Rectal Surg*. 2014;27(4):125–133.
38. Singer AJ, Clark RA. Cutaneous wound healing. *N Engl J Med*. 1999;341(10):738–746.
39. Schaffer M, Barbul A. Lymphocyte function in wound healing and following injury. *Br J Surg*. 1998;85(4):444–460.
40. Nordentoft T, Pommegaard HC, Rosenberg J, Achiam MP. Fibrin glue does not improve healing of gastrointestinal anastomoses: a systematic review. *Eur Surg Res*. 2015;54(1–2):1–13.
41. Vakalopoulos KA, Daams F, Wu Z, Timmermans L, Jeekel JJ, Kleinrensink GJ, van der Ham A, Lange JF. Tissue adhesives in gastrointestinal anastomosis: a systematic review. *J Surg Res*. 2013;180(2):290–300.
42. Sliker JC, Vakalopoulos KA, Komen NA, Jeekel J, Lange JF. Prevention of leakage by sealing colon anastomosis: experimental study in a mouse model. *J Surg Res*. 2013;184(2):819–824.
43. Wu Z, Boersema GS, Kroese LF, Taha D, Vennix S, Bastiaansen-Jenniskens YM, Lam KH, Kleinrensink GJ, Jeekel J, Pelpelenbosch M, et al. Reducing colorectal anastomotic leakage with tissue adhesive in experimental inflammatory bowel disease. *Inflamm Bowel Dis*. 2015;21(5):1038–1046.
44. Baum ML, Anish DS, Chalmers TC, Sacks HS, Smith H, Jr, Fagerstrom RM. A survey of clinical trials of antibiotic prophylaxis in colon surgery: evidence against further use of no-treatment controls. *N Engl J Med*. 1981;305(14):795–799.
45. Fry DE. Antimicrobial bowel preparation for elective colon surgery. *Surg Infect (Larchmt)*. 2016;17(3):269–274.
46. Irkorucu O, Ucan BH, Cakmak GK, Emre AU, Tascilar O, Ofloglu E, Bahadir B, Karakaya K, Demirtas C, Ankarali H, et al. Does sildenafil reverse the adverse effects of ischemia on ischemic colon anastomosis: yes, ‘no’. *Int J Surg*. 2009;7(1):39–43.
47. Semont A, Demarquay C, Bessout R, Durand C, Benderitter M, Mathieu N. Mesenchymal stem cell therapy stimulates endogenous host progenitor cells to improve colonic epithelial regeneration. *PLoS One*. 2013;8(7):e70170.
48. Linard C, Busson E, Holler V, Strup-Perrot C, Lacave-Lapalun JV, Lhomme B, Prat M, Devauchelle P, Sabourin JC, Simon JM, et al. Repeated autologous bone marrow-derived mesenchymal stem cell injections improve radiation-induced proctitis in pigs. *Stem Cells Transl Med*. 2013;2(11):916–927.
49. Liu L, Chiu PW, Lam PK, Poon CC, Lam CC, Ng EK, Lai PB. Effect of local injection of mesenchymal stem cells on healing of sutured gastric perforation in an experimental model. *Br J Surg*. 2015;102(2):e158–e168.
50. Lee RH, Pulin AA, Seo MJ, Kota DJ, Ylostalo J, Larson BL, Semprun-Prieto L, Delafontaine P, Prockop DJ. Intravenous hMSCs improve myocardial infarction in mice because cells embolized in lung are activated to secrete the anti-inflammatory protein TSG-6. *Cell Stem Cell*. 2009;5(1):54–63.
51. Hauer-Jensen M, Wang J, Boerma M, Fu Q, Denham JW. Radiation damage to the gastrointestinal tract: mechanisms, diagnosis, and management. *Curr Opin Support Palliat Care*. 2007;1(1):23–29.
52. Chang P, Qu Y, Liu Y, Cui S, Zhu D, Wang H, Jin X. Multi-therapeutic effects of human adipose-derived mesenchymal stem cells on radiation-induced intestinal injury. *Cell Death Dis*. 2013;4:e685.
53. Gremy O, Benderitter M, Linard C. Acute and persisting Th2-like immune response after fractionated colorectal gamma-irradiation. *World J Gastroenterol*. 2008;14(46):7075–7085.
54. Moussa L, Pattappa G, Doix B, Benselama SL, Demarquay C, Benderitter M, Semont A, Tamarat R, Guicheux J, Weiss P, et al. A biomaterial-assisted mesenchymal stromal cell therapy alleviates colonic radiation-induced damage. *Biomaterials*. 2017;115:40–52.